

SPACECRAFT ATTITUDE MOTION PLANNING ON SO(3) USING GRADIENT-BASED OPTIMIZATION

Fabio Celani^{*} and Dennis Lucarelli[†]

The purpose of the present work is to perform spacecraft attitude motion planning so that a rest-to-rest rotation is achieved while satisfying pointing constraints. Attitude is represented on the group of three dimensional rotations SO(3). The motion planning is executed in two steps. In the first step, path-planning is performed by searching for a time behavior for the angular rates through the formulation of an optimal control problem solved with a gradient-based algorithm. In the second step, the actual input torque is simply determined by the use of inverse attitude dynamics. A numerical example is included to show the effectiveness of the method. From a practical point of view, the control torque resulting from the proposed approach is continuously differentiable and vanishes at its endpoints.

INTRODUCTION

Attitude motion planning is necessary in mission scenarios in which the spacecraft must perform large angle maneuvers with the additional requirement that sensitive instruments must not point to bright objects such as Sun, Moon, and Earth. These so-called “keep-out cones” define constraints that must be satisfied along the instrument trajectory. This research presents a control synthesis method for constructing an appropriate control torque that achieves the desired rest-to-rest maneuver and ensures that the keep-out cones are avoided.

In this work, the spacecraft attitude is globally represented on the special orthogonal group SO(3). Performing motion planning on SO(3) carries benefits over representations such as Euler angles (e.g. References 1 and 2) and quaternions (e.g. References 3–6). In fact, Euler angles are defined only locally and exhibit kinematic singularities which can limit the width of the maneuvers. On the other hand, quaternions do not possess singularities and are often used in spacecraft attitude motion planning. However, they have ambiguities in representing attitude since the three-dimensional sphere double covers SO(3). Thus, since boundary conditions for the spacecraft attitude do not have a unique representation in quaternions, a quaternion-based motion planning may exhibit the unwinding behavior.⁷ Moreover, the proposed method presents the following advantages compared to other approaches for spacecraft motion planning on SO(3). It is simpler to implement than the algorithm in Reference 8 since it does not require either randomization or discretization tools. It is easier to use with respect to the approach in Reference 9 since it does not ask for geometric visual inspection to perform path-planning. In addition, the proposed algorithm naturally handles limits on the control torque amplitude unlike Reference 10. From a practical point of view, the control torque

^{*} Assistant Professor, School of Aerospace Engineering, Sapienza University of Rome, Via Salaria 851 00138 Roma Italy. E-mail: E-mail: fabio.celani@uniroma1.it.

[†] Research Associate Professor, Department of Physics, American University, 4400 Massachusetts Ave NW, Washington, DC 20016. E-mail: dgl@american.edu.

resulting from the proposed approach is continuously differentiable and vanishes at its endpoints. Thus, it is easier to implement on real spacecraft than time-optimal control torques that often do not vanish at endpoints and are sometimes discontinuous during the maneuver.^{3,5,6}

The proposed method consists of two steps. In the first, path-planning is performed to determine an appropriate time behavior for the angular rate so that the spacecraft is reoriented to the desired attitude while avoiding exclusion cones. Since in the path-planning problem the state space is the Lie group SO(3), its solution can be obtained by adapting a recent method for control synthesis on Lie groups originally used for quantum mechanical systems and known as “Gradient Ascent in Function Space” (GRAFS).¹¹ In the second step, known as motion planning, the actual control torque is simply determined by the use of inverse attitude dynamics. As in Reference 9, a time scaling is introduced to reduce the torque amplitude to within the allowed limits.

The rest of the paper is organized as follows. In the next section, the attitude motion planning problem is formulated. The following section describes how the path-planning problem can be solved through a gradient-based optimization approach. Next, the motion planning method is presented. The proposed method is then validated through a case study inspired by a real-world problem. Conclusions are drawn in the last section.

PROBLEM STATEMENT

In the spacecraft attitude motion planning problem on SO(3), the initial attitude $R_i \in \text{SO}(3)$ and the desired final attitude $R_f \in \text{SO}(3)$ are given, and both the initial angular velocity and the desired final angular velocity must be zero (rest-to-rest maneuver). The attitude $R(t) \in \text{SO}(3)$ is subject to the kinematic constraint

$$\dot{R}(t) = R(t) \Omega(t) \quad (1)$$

where

$$\Omega(t) = \omega_1(t)A_1 + \omega_2(t)A_2 + \omega_3(t)A_3 \quad (2)$$

in which ω_1 , ω_2 , and ω_3 are the components of the spacecraft angular velocity along body axes. Matrices A_1 , A_2 , and A_3 form a basis for the Lie algebra corresponding to SO(3) and are given by

$$A_1 = \begin{bmatrix} 0 & 0 & 0 \\ 0 & 0 & -1 \\ 0 & 1 & 0 \end{bmatrix} \quad A_2 = \begin{bmatrix} 0 & 0 & 1 \\ 0 & 0 & 0 \\ -1 & 0 & 0 \end{bmatrix} \quad A_3 = \begin{bmatrix} 0 & -1 & 0 \\ 1 & 0 & 0 \\ 0 & 0 & 0 \end{bmatrix}$$

The relation between $\omega = [\omega_1 \ \omega_2 \ \omega_3]^T$ and the control torque resolved in body frame T is given by the well-known Euler equation

$$J\dot{\omega} + \omega \times J\omega = T \quad (3)$$

in which J is the spacecraft inertia matrix. Denote with \bar{T} the maximum amplitude of T_j $j = 1, 2, 3$ due to actuator constraints.

The spacecraft is equipped with an on-board sensor whose pointing direction in body coordinates is given by unit vector r . There are C undesired pointing directions for the sensor which are specified in inertial coordinates by unit vectors w_i $i = 1, \dots, C$. For example, r can be the pointing direction of an on-board optical sensor, and w_i is the inertial direction of a bright celestial object. It is required that the boresight of the sensor avoids inertial direction w_i with a minimum offset angle $0 < \theta_i < 90^\circ$. Thus, the following constraints are introduced

$$r^T R(t)^T w_i \leq \cos \theta_i \quad i = 1, \dots, C \quad (4)$$

Given the initial conditions $R(0) = R_i$ $\omega(0) = 0$, the objective is to determine a torque input $T(t)$ defined over a finite interval $[0 \ t_f]$ that fulfills the amplitude constraint

$$|T_j(t)| \leq \bar{T} \quad j = 1, 2, 3 \quad 0 \leq t \leq t_f \quad (5)$$

and is such that the corresponding attitude $R(t)$ and attitude rate $\omega(t)$ satisfy the final conditions $R(t_f) = R_f$ $\omega(t_f) = 0$, and the pointing constraints (4) for all $0 \leq t \leq t_f$.

PATH-PLANNING USING GRADIENT-BASED OPTIMIZATION

Path-planning consists in finding an appropriate time behavior for the attitude rate so that the spacecraft is reoriented to the desired attitude while avoiding exclusion cones. Thus, in this first phase, only attitude kinematics in Eq. (1) are considered, and the angular rate $\omega = [\omega_1 \ \omega_2 \ \omega_3]^T$ is seen as control input. In this phase, a normalized time $0 \leq \tau \leq 1$ is adopted. This is equivalent to setting the final time $t_f = 1$ in which case $t = \tau$.

In this paper, the path-planning is performed first by expressing the angular rate as follows

$$\omega_j(\tau) = \sum_{k=1}^M \alpha_{jk} v_k(\tau) \quad j = 1, 2, 3 \quad (6)$$

for a set of M basis functions $v_k(\tau)$ $k = 1, \dots, M$. The basis functions must fulfill the following end-point conditions $v_k(0) = v_k(1) = 0$ $k = 1, \dots, M$ so that $\omega(0) = \omega(1) = 0$ as required.

The path-planning problem is formulated as an optimization problem in which the decision variables are the weights α_{jk} in the expansion in Eq. (6). The objective function to be minimized is chosen as

$$\frac{1}{2} \sum_{j=1}^3 \sum_{k=1}^M \alpha_{jk}^2 \quad (7)$$

so to reduce, to a certain extent, the amplitude of the angular rate $\omega(\tau)$. This in turn will reduce the spacecraft maneuvering time as it will be explained in the following section on motion planning. Moreover, if the basis functions $v_k(\tau)$ $k = 1, \dots, M$ are orthonormal

$$\int_0^1 v_m(\tau) v_n(\tau) d\tau = \begin{cases} 1 & \text{if } m = n \\ 0 & \text{if } m \neq n \end{cases}$$

then, minimizing the objective function is equivalent to minimizing the “energy” of the signal $\omega(\tau)$ given by

$$\int_0^1 \|\omega(\tau)\|^2 d\tau$$

Achieving the desired final attitude is enforced through the following equality constraint

$$\text{tr} [R_f^T R(1)] = 3 \quad (8)$$

where tr denotes the trace of a matrix. In addition, exclusion cones are avoided by adding the inequality constraints (4).

Thus, the optimization problem becomes

$$\begin{aligned} \underset{\alpha_{jk}}{\text{minimize}} \quad & \frac{1}{2} \sum_{j=1}^3 \sum_{k=1}^M \alpha_{jk}^2 \\ \text{subject to} \quad & \frac{dR}{d\tau}(\tau) = R(\tau) \Omega(\tau) \\ & \text{tr}[R_f^T R(1)] = 3 \\ & r^T R(\tau)^T w_i \leq \cos \theta_i \end{aligned} \quad (9)$$

with $0 \leq \tau \leq 1$ $i = 1, \dots, C$. The optimization problem is solved numerically by adopting the following approach. Discretize the interval $[0, 1]$ into N equal segments defining $\Delta\tau = 1/N$ and $\tau_\ell = (\ell - 1)\Delta\tau$ $\ell = 1, \dots, N + 1$. Inequality constraints are enforced only at the discrete times τ_ℓ $\ell = 1, \dots, N + 1$ obtaining

$$r^T R(\tau_\ell)^T w_i \leq \cos \theta_i \quad \ell = 1, \dots, N + 1 \quad i = 1, \dots, C \quad (10)$$

Moreover, $R(\tau_\ell)$ is computed through the following approximation. Consider the infinitesimal rotations

$$P(\tau_\ell) = \exp[\omega_1(\tau_\ell)\Delta\tau A_1 + \omega_2(\tau_\ell)\Delta\tau A_2 + \omega_3(\tau_\ell)\Delta\tau A_3] \quad \ell = 1, \dots, N$$

The solution to Eq. (1) is approximated by the following product

$$R(\tau_\ell) \approx R_i P(\tau_1) \cdots P(\tau_{\ell-1}) = R_i \left(\prod_{q=1}^{\ell-1} P(\tau_q) \right) \quad \ell = 2, \dots, N + 1 \quad (11)$$

In addition, note that $R(\tau_1) = R(0) = R_i$. This approximate solution enforces the time ordering of the general solution to Eq. (1) but retains only the first order term in the Magnus expansion of the matrix exponential, and represents the exact solution of (1) when $\omega(\tau)$ is approximated through a zero-order-hold operation. The approximation in Eq. (11) is employed also to compute $R(1)$ appearing in the equality constraint.

To solve the optimization problem thus formulated using steepest descent methods, analytical expressions for the gradients of the constraints in Eqs. (8) and (10) with respect to weights α_{jk} must be provided. First note that weights α_{jk} affect the constraints only through $R(\tau_\ell)$. Define

$$P_{i:j} = \begin{cases} \prod_{\ell=i}^j P(\tau_\ell) & \text{if } i \leq j \\ I_{3 \times 3} & \text{if } i > j \end{cases}$$

then the following holds

$$\begin{aligned} \frac{\partial R(\tau_\ell)}{\partial \alpha_{jk}} & \approx R_i \frac{\partial [P(\tau_1) \cdots P(\tau_{\ell-1})]}{\partial \alpha_{jk}} \\ & = R_i \left(\sum_{q=1}^{\ell-1} P_{1:q-1} \frac{\partial P(\tau_q)}{\partial \alpha_{jk}} P_{q+1:N} \right) \quad j = 1, 2, 3 \quad k = 1, \dots, M \quad \ell = 2, \dots, N + 1 \end{aligned} \quad (12)$$

Since a variation in a weight α_{jk} affects the variable $\omega_j(\tau)$ at all times, and in particular affects $\omega_j(\tau_q)$, then the following holds true

$$\frac{\partial P(\tau_q)}{\partial \alpha_{jk}} = \frac{\partial P(\tau_q)}{\partial \omega_j(\tau_q)} \frac{\partial \omega_j(\tau_q)}{\partial \alpha_{jk}} = v_k(\tau_q) \frac{\partial P(\tau_q)}{\partial \omega_j(\tau_q)} \quad q = 1, \dots, N \quad j = 1, 2, 3 \quad k = 1, \dots, M \quad (13)$$

The last partial derivative in the previous equation can be computed as follows. Let $\lambda_i \ i = 1, 2, 3$ be the eigenvalues of $\Omega(\tau_q)$ (see Eq. (2)) and $u_i \in \mathbb{R}^3 \ i = 1, 2, 3$ be the corresponding eigenvectors having unit norm. Since $\Omega(\tau_q)$ is skew-symmetric of dimension three, then it has a zero eigenvalue and the other two are imaginary conjugate. Moreover, the 3×3 complex matrix

$$U \triangleq [u_1 \ u_2 \ u_3]$$

is a unitary matrix since it satisfies $U^\dagger U = UU^\dagger = I_{3 \times 3}$ where U^\dagger denotes the conjugate transpose of U and $I_{3 \times 3}$ is the three-dimensional identity matrix.. The following result can then be stated.

Proposition 1. *It holds that*

$$\frac{\partial P(\tau_q)}{\partial \omega_j(\tau_q)} = U E U^\dagger \quad (14)$$

where E is a 3×3 complex matrix defined by

$$E_{mn} \triangleq \begin{cases} \Delta\tau u_m^\dagger A_j u_m e^{\Delta\tau\lambda_m} & \text{for } \lambda_m = \lambda_n \\ u_m^\dagger A_j u_n \frac{e^{\Delta\tau\lambda_n} - e^{\Delta\tau\lambda_m}}{\lambda_n - \lambda_m} & \text{for } \lambda_m \neq \lambda_n \end{cases} \quad (15)$$

Proof. See Appendix □

As a result, analytical expressions for the gradients of constraints (8) and (10) based on approximation (11) can be obtained by using Eqs. (12)-(15).

MOTION PLANNING

The output of the path-planning phase is the time behavior $\omega^*(\tau) \ 0 \leq \tau \leq 1$ which fulfills $\omega^*(0) = \omega^*(1) = 0$, and possesses the following property: let $R^*(\tau)$ be the corresponding time behavior for the attitude subject to the initial condition $R^*(0) = R_i$. Clearly $R^*(\tau)$ fulfills the pointing constraints in Eq. (4), as well as the final condition $R^*(1) = R_f$ if the number of time segments N is large enough so that approximation in Eq.(11) is sufficiently accurate. The required torque can be obtained from the attitude dynamics (3) as

$$T^*(\tau) = J \frac{d\omega^*}{d\tau}(\tau) + \omega^*(\tau) \times J\omega^*(\tau) \quad 0 \leq \tau \leq 1 \quad (16)$$

The control torque $T^*(\tau)$ may not fulfill the amplitude constraints $|T_j^*(\tau)| \leq \bar{T} \ 0 \leq \tau \leq 1 \ j = 1, 2, 3$. In that case, the time scaling $t = t_f \tau$ is performed in which $t_f > 1$ is chosen to reduce speed at which the path in $\text{SO}(3)$ is traced out, and consequently to have the torque amplitude within the prescribed limits. Specifically, consider $R(t) = R^*(t/t_f) \ 0 \leq t \leq t_f$. Clearly, $R(t)$ fulfills the pointing constraints in Eq. (4) as well as the initial and final conditions $R(0) = R_i$, $R(t_f) = R_f$. Then, it is immediate to see that the angular velocity in the scaled time t is given by

$\omega(t) = 1/t_f \omega^*(t/t_f)$ $0 \leq t \leq t_f$ which satisfies $\omega(0) = \omega(t_f) = 0$. Moreover, it is easy to obtain that the input torque is equal to

$$T(t) = \frac{1}{t_f^2} T^* \left(\frac{t}{t_f} \right) \quad 0 \leq t \leq t_f \quad (17)$$

Thus, t_f must be selected larger than 1 so that torque $T(t)$ satisfies the amplitude constraint in Eq. (5). On the other hand, if the amplitude of $T^*(\tau)$ is below its limits, then t_f can be reduced to a value less than 1.

From Eqs. (16) and (17) it appears that intuitively the smaller the amplitude of ω^* , the smaller t_f that ensures the satisfaction of the amplitude constraint on $T(t)$. Since adopting the cost function in Eq. (7) is equivalent to a certain extent, to minimizing the amplitude of ω^* , such cost function leads to an approximate minimization of the maneuvering time t_f .

CASE STUDY

We demonstrate the proposed approach through a case study formulated in References 6 and 12, and inspired by a maneuver performed by the Swift spacecraft. Consider a spacecraft that has to perform a rest-to rest maneuver consisting of a rotation of $3/4\pi$ rad about its z -axis. Thus, setting the initial attitude as $R_i = I_{3 \times 3}$, the desired final attitude is equal to

$$R_f = \begin{bmatrix} \cos(3/4\pi) & -\sin(3/4\pi) & 0 \\ \sin(3/4\pi) & \cos(3/4\pi) & 0 \\ 0 & 0 & 1 \end{bmatrix}$$

The spacecraft is equipped with a sensor whose axis has coordinates $r = [1 \ 0 \ 0]^T$ in body frame. The following three keep-out cones must be avoided by the sensor during the manouevre:

- Sun cone with inertial direction $w_1 = [0.5 \ 0.866 \ 0]^T$ and minimum offset angle $\theta_1 = 47$ deg;
- Earth cone with inertial direction $w_2 = [0 \ 0 \ -1]^T$ and minimum offset angle $\theta_2 = 33$ deg;
- Moon cone with inertial direction $w_3 = [0.1795 \ 0.3109 \ 0.9333]^T$ and minimum offset angle $\theta_3 = 23$ deg.

There is a gap of 10 deg between the Sun and Earth cones but no gap between the Sun and Moon cones (see Fig. 1).

The optimization problem in Eq. (9) is solved by using the numerical approach previously discussed. Consequently, it is enough to select samples $v_k(\tau_\ell)$ $k = 1, \dots, M$ $\ell = 1, \dots, N$ rather than the whole continuous-time basis functions $v_k(\tau)$ $k = 1, \dots, M$ since only the samples appear in the equality and inequality constraints. In this example $v_k(\tau_\ell)$ are chosen as the so-called Slepian sequences.¹³ These sequences, commonly used in spectrum estimation and signal processing, are parameterized by their length N and the half-bandwidth parameter $W \in [0 \ 0.5]$. In this case study, the first $M = 4$ Slepian sequences with $N = 500$ and $W = 0.015$ have been considered. The corresponding time behaviors are reported in Fig. 2 and show that $v_k(0) \simeq 0$, $dv_k/d\tau(0) \simeq 0$, $v_k(1) \simeq 0$, $dv_k/d\tau(1) \simeq 0$. As a result, by Eq. (6), the following holds

$$\omega(0) \simeq 0 \quad \frac{d\omega}{d\tau}(0) \simeq 0 \quad \omega(1) \simeq 0 \quad \frac{d\omega}{d\tau}(1) \simeq 0 \quad (18)$$

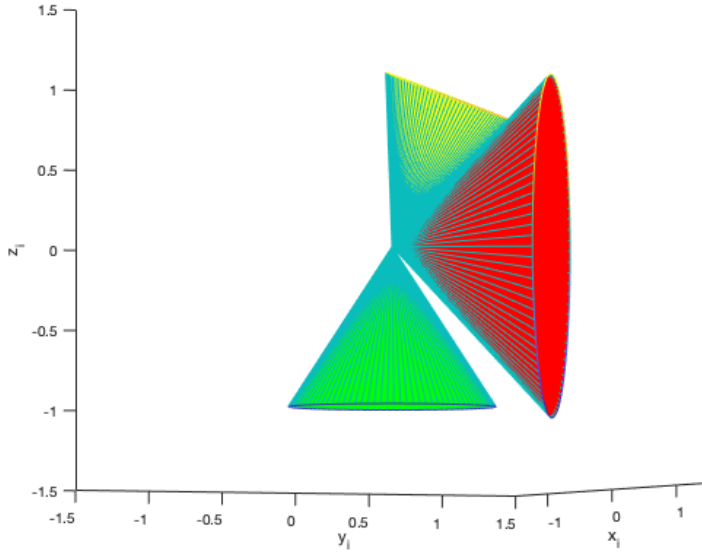


Figure 1. Sun cone (red), Earth cone (green), Moon cone (yellow).

ensuring that a rest-to-rest maneuver is obtained. To determine for the values of the weights α_{jk} $j = 1, \dots, 3$ $k = 1, \dots, 4$, the nonlinear programming problem in Eq. (9) is solved numerically using a local, gradient-based interior point method¹⁴ implemented in Scientific Python.¹⁵ Note that the cost function in Eq. (7) naturally leads to setting $\alpha_{jk} = 0$ as the initial guess for the interior point algorithm. The outcome of the path-planning step is given by the time samples of the angular-rate in normalized time $\omega^*(\tau_\ell)$ $\ell = 1, \dots, 500$ which are represented in Figure 3. Samples of the torque expressed in normalized time $T^*(\tau_\ell)$ $\ell = 1, \dots, 500$ can be obtained by using Eq. (16) by adopting the following finite difference approximation

$$\frac{d\omega^*}{d\tau}(\tau_\ell) \simeq \begin{cases} 0 & \text{for } \ell = 1 \\ \frac{\omega^*(\tau_\ell) - \omega^*(\tau_{\ell-1})}{\tau_\ell - \tau_{\ell-1}} & \text{for } \ell = 2, \dots, 500 \end{cases}$$

As in Reference 6, consider an isoinertial spacecraft so that $J = J_0 I_{3 \times 3}$. The corresponding time behavior of $T^*(\tau_\ell)/J_0$ $\ell = 1, \dots, 500$ is represented in Fig. 4.

By Eq. (17), samples of the physical control torque are obtained as follows

$$T(t_\ell) = \frac{1}{t_f^2} T^*(\tau_\ell) \quad \ell = 1, \dots, N$$

where t_f is the physical final time and $t_\ell = t_f \tau_\ell$ $\ell = 1, \dots, 500$. Time t_f is chosen so that

$$|T_j(t_\ell)| \leq \bar{T} \quad j = 1, 2, 3 \quad \ell = 1, \dots, 500 \quad (19)$$

Let

$$\bar{T}^*/J_0 = \max_{j,\ell} |T_j^*(\tau_\ell)/J_0|$$

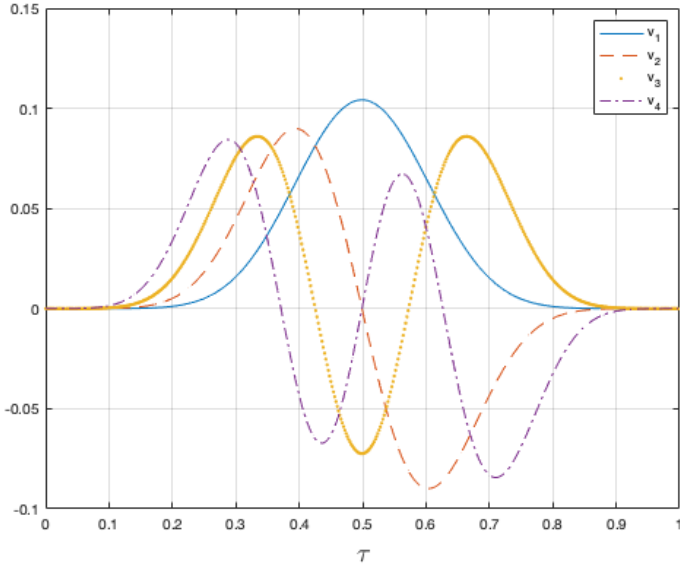


Figure 2. Samples of basis functions $v_k(\tau_\ell)$ $k = 1, \dots, 4$ $\ell = 1, \dots, 500$.

It turns out that $\overline{T^*}/J_0 = 40.53$. Introduce time unit $\text{TU} = \sqrt{J_0/\overline{T}}$, then it is easy to see that the value $t_f = \text{TU}\sqrt{\overline{T^*}/J_0} = 6.37$ TU guarantees that Eq. (19) is fulfilled as confirmed by Fig. 5. The continuous time control torque $T(t)$ $0 \leq t \leq t_f$ is then simply obtained from the samples $T(\tau_\ell)$ through a zero-order hold operation. Fig. 5 shows that, from a practical point of view, $T(t)$ can be considered continuously differentiable and vanishing at its endpoints. Both properties are consequences of our choice for the samples $v_k(\tau_\ell)$ (see Figure 2). In particular, $T(t)$ vanishes at its endpoints as a consequence of the properties in Eq. (18). Since $T(t)$ is continuously differentiable and vanishes at its end-points, its implementation on real spacecraft is easier compared to time-optimal control torques that often do not vanish at endpoints and are sometimes discontinuous during the maneuver.^{3,5,6}

To validate the effectiveness of the obtained input torque, Eqs. (1)-(3) with the appropriate initial conditions $R(0) = I_{3 \times 3}$ $\omega(0) = 0$ are integrated numerically and the following results are obtained. The obtained final attitude $R(t_f)$ satisfies the following

$$3 - \text{tr}[R_f^T R(t_f)] = 1.51 \cdot 10^{-10}$$

and $\|\omega(t_f)\| = 9.22 \cdot 10^{-7}$ which implies that the spacecraft reaches the desired final attitude R_f with zero angular velocity. The time behaviors of

$$c_i(t) = r^T R(t)^T w_i - \cos \theta_i \quad i = 1, 2, 3$$

are shown in Fig. 6 confirming that the three pointing constraints are fulfilled. The path of the sensitive direction, the three exclusion cones, the initial and the desired final sensitive directions are all displayed in Fig. 7. By inspection the proposed method leads to a solution that apparently minimizes the length of the path.

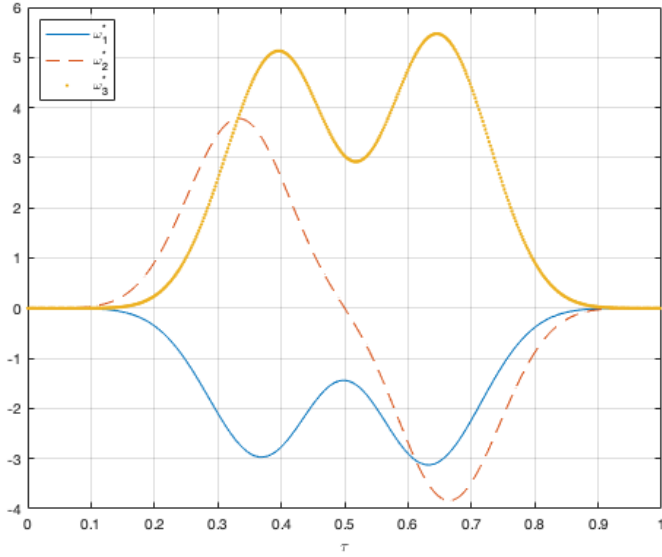


Figure 3. Samples $\omega^*(\tau_\ell)$ $\ell = 1, \dots, 500$.

A time-optimal approach to the same attitude motion planning problem is presented in Reference 6 and achieves a maneuvering time of about 3.5 TU. The method proposed here does not explicitly minimize time and performs the maneuver in 6.37 TU which is substantially longer. However, our approach leads to a control torque that vanishes at its endpoints (see Fig. 5) making it easier to implement on real spacecraft compared to the control torque in Figure 26 of Reference 6.

CONCLUSION

The spacecraft attitude motion planning approach presented in this work provides a systematic method for performing rest-to-rest maneuvers taking into account multiple pointing constraints. It possesses the important feature of representing attitude on the special orthogonal group $\text{SO}(3)$ thus avoiding singularities and ambiguities associated with other attitude representations. Compared to other methods that are based on the same attitude representation, the proposed method is simpler and more systematic. Moreover, it can provide a control torque that vanishes at its endpoints. The latter is simpler to implement than control torques determined through a time-optimal approach.

APPENDIX

Proof of Proposition 1

Clearly, Eq. (14) is equivalent to

$$E = U^\dagger \frac{\partial P(\tau_q)}{\partial \omega_j(\tau_q)} U$$

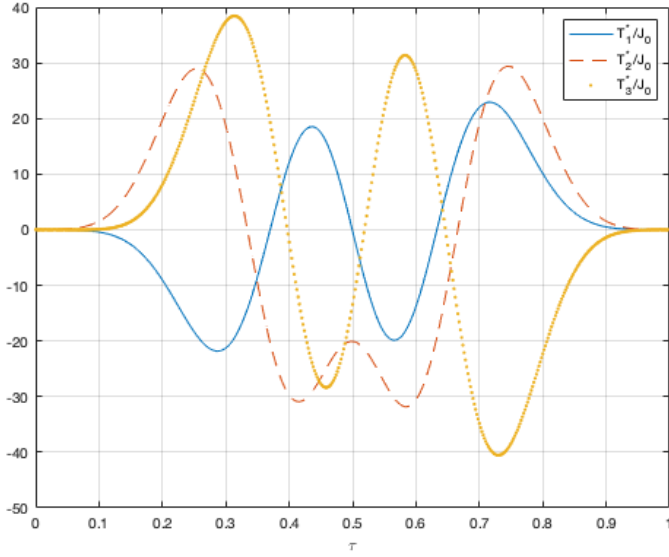


Figure 4. Samples $T^*(\tau_\ell)/J_0 \ell = 1, \dots, 500$.

which is equivalent to

$$E_{m n} = u_m^\dagger \frac{\partial P(\tau_q)}{\partial \omega_j(\tau_q)} u_n \quad m, n = 1, 2, 3 \quad (20)$$

Note that

$$\begin{aligned} \frac{\partial P(\tau_q)}{\partial \omega_j(\tau_q)} &= \frac{\partial}{\partial \omega_j(\tau_q)} \exp \left(\sum_{\nu=1}^3 \omega_\nu(\tau_q) \Delta \tau A_\nu \right) \\ &= \left\{ \frac{\partial}{\partial x} \exp \left[(\omega_j(\tau_q) + x) \Delta \tau A_j + \sum_{\substack{\nu=1 \\ \nu \neq j}}^3 \omega_\nu(\tau_q) \Delta \tau A_\nu \right] \right\}_{x=0} \\ &= \left\{ \frac{\partial}{\partial x} \exp [\Omega(\tau_q) \Delta \tau + x \Delta \tau A_j] \right\}_{x=0} \end{aligned}$$

Thus

$$u_m^\dagger \frac{\partial P(\tau_q)}{\partial \omega_j(\tau_q)} u_n = u_m^\dagger \left\{ \frac{\partial}{\partial x} \exp [\Omega(\tau_q) \Delta \tau + x \Delta \tau A_j] \right\}_{x=0} u_n \quad (21)$$

Clearly, the eigenvalues of matrix $\Omega(\tau_q) \Delta \tau$ are given by $\lambda_i \Delta \tau \ i = 1, 2, 3$, and it is immediate to verify that the corresponding eigenvectors with unit norm are given by $u_i \ i = 1, 2, 3$. Using

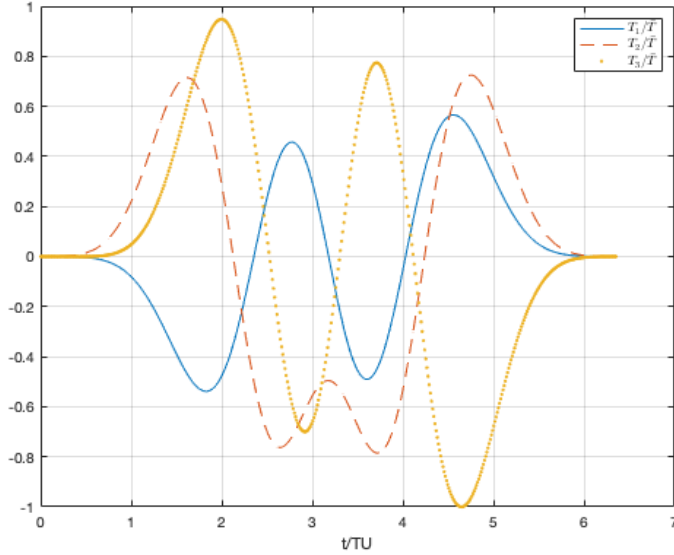


Figure 5. Samples $T(t_\ell)/\bar{T}$ $\ell = 1, \dots, 500$.

Theorem 1, obtain the following

$$u_m^\dagger \left\{ \frac{\partial}{\partial x} \exp [\Omega(\tau_q) \Delta \tau + x \Delta \tau A_j] \right\}_{x=0} u_n = \begin{cases} \Delta \tau u_m^\dagger A_j u_m e^{\Delta \tau \lambda_m} & \text{for } \lambda_m = \lambda_n \\ u_m^\dagger A_j u_n \frac{e^{\Delta \tau \lambda_n} - e^{\Delta \tau \lambda_m}}{\lambda_n - \lambda_m} & \text{for } \lambda_m \neq \lambda_n \end{cases} \quad (22)$$

Thus, taking into account of Eq. (15), the equality in Eq. (20) is a direct consequence of Eqs. (21) and (22).

A Spectral Theorem

Theorem 1. Let A and B be $l \times l$ skew-Hermitian complex matrices (i.e. $A^\dagger = -A, B^\dagger = -B$). Denote the eigenvalues of A by λ_i $i = 1, \dots, l$, and let $u_i \in \mathbb{R}^l$ $i = 1, \dots, l$ be the corresponding eigenvectors having unit norm. Let $x \in \mathbb{R}$, then for any $m, n = 1, \dots, l$ the following holds

$$u_m^\dagger \left[\frac{\partial}{\partial x} \exp (A + xB) \right]_{x=0} u_n = \begin{cases} u_m^\dagger B u_m e^{\lambda_m} & \text{for } \lambda_m = \lambda_n \\ u_m^\dagger B u_n \frac{e^{\lambda_n} - e^{\lambda_m}}{\lambda_n - \lambda_m} & \text{for } \lambda_m \neq \lambda_n \end{cases}$$

Proof. See Appendix A of Reference 16. \square

REFERENCES

- [1] H. Hablani, “Attitude commands avoiding bright objects and maintaining communication with ground station,” *Journal of Guidance, Control, and Dynamics*, Vol. 22, No. 6, 1999, pp. 759–767.
- [2] C. McInnes, “Large angle slew maneuvers with autonomous sun vector avoidance,” *Journal of Guidance, Control, and Dynamics*, Vol. 17, No. 4, 1994, pp. 875–877, 10.2514/3.21283.

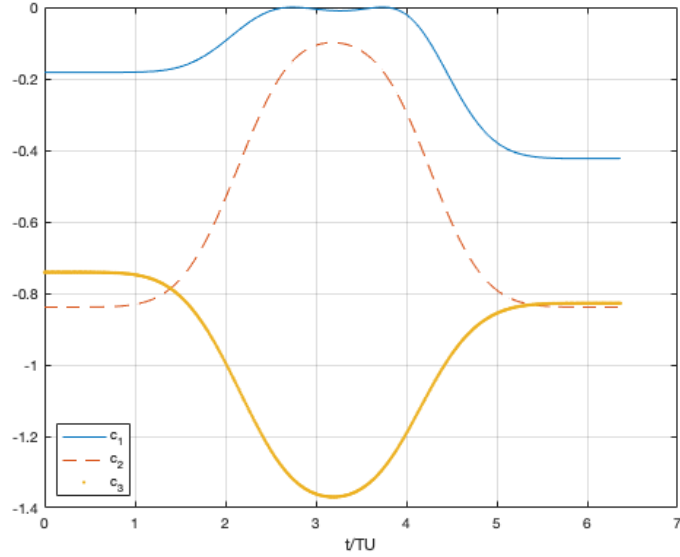


Figure 6. Pointing constraints.

- [3] G. Boyarko, M. Romano, and O. Yakimenko, “Time-optimal reorientation of a spacecraft using an inverse dynamics optimization method,” *Journal of Guidance, Control, and Dynamics*, Vol. 34, No. 4, 2011, pp. 1197–1208.
- [4] H. Kjellberg and E. Lightsey, “Discretized constrained attitude pathfinding and control for satellites,” *Journal of Guidance, Control, and Dynamics*, Vol. 36, No. 5, 2013, pp. 1301–1309. cited By 18, 10.2514/1.60189.
- [5] D. Spiller, L. Ansalone, and F. Curti, “Particle swarm optimization for time-optimal spacecraft reorientation with keep-out cones,” *Journal of Guidance, Control, and Dynamics*, Vol. 39, No. 2, 2016, pp. 312–325.
- [6] R. Melton, “Differential evolution/particle swarm optimizer for constrained slew maneuvers,” *Acta Astronautica*, Vol. 148, 2018, pp. 246–259.
- [7] N. A. Chaturvedi, A. K. Sanyal, and N. H. McClamroch, “Rigid-body attitude control,” *IEEE Control Systems Magazine*, Vol. 31, June 2011, pp. 30–51.
- [8] E. Frazzoli, M. Dahleh, E. Feron, and R. Kornfeld, “A randomized attitude slew planning algorithm for autonomous spacecraft,” *AIAA Guidance, Navigation, and Control Conference and Exhibit*, AIAA Paper 2001-4155, 2001.
- [9] J. Biggs and L. Colley, “Geometric attitude motion planning for spacecraft with pointing and actuator constraints,” *Journal of Guidance, Control, and Dynamics*, Vol. 39, No. 7, 2016, pp. 1669–1674.
- [10] T. Lee, “Geometric tracking control of the attitude dynamics of a rigid body on $\text{SO}(3)$,” *Proceedings of the 2011 American Control Conference*, June 2011, pp. 1200–1205.
- [11] D. Lucarelli, “Quantum optimal control via gradient ascent in function space and the time-bandwidth quantum speed limit,” *Physical Review A*, Vol. 97, No. 6, 2018.
- [12] M. Pontani and R. Melton, “Heuristic optimization of satellite reorientation maneuvers,” *AIAA/AAS Astrodynamics Specialist Conference*, 2016.
- [13] D. Slepian, “Prolate Spheroidal Wave Functions, Fourier Analysis, and Uncertainty—V: The Discrete Case,” *Bell Syst. Tech. J.*, Vol. 57, 1978, pp. 1371–1430.
- [14] R. H. Byrd, M. E. Hribar, and J. Nocedal, “An interior point algorithm for large-scale nonlinear programming,” *SIAM Journal on Optimization*, Vol. 9, No. 4, 1999, pp. 877–900.
- [15] T. E. Oliphant, “Python for scientific computing,” *Computing in Science & Engineering*, Vol. 9, No. 3, 2007.

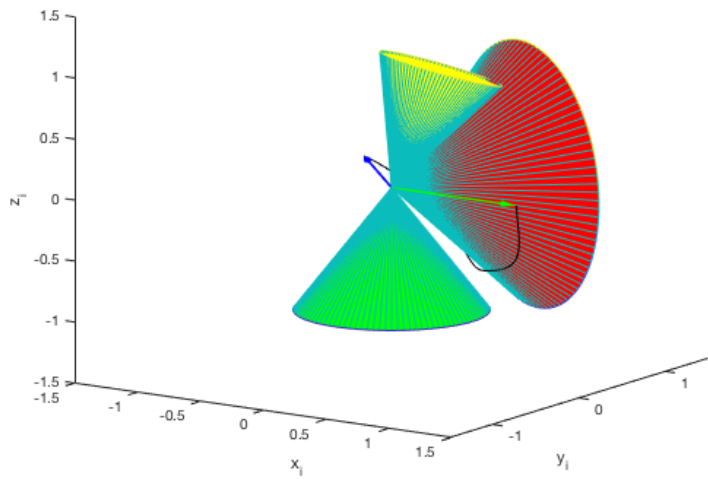


Figure 7. Path of sensitive direction (black curve), exclusion cones, initial sensitive direction (green arrow), desired final sensitive direction (blue arrow).

- [16] S. Machnes, U. Sander, S. Glaser, P. De Fouquière, A. Gruslys, S. Schirmer, and T. Schulte-Herbrüggen, “Comparing, optimizing, and benchmarking quantum-control algorithms in a unifying programming framework,” *Physical Review A - Atomic, Molecular, and Optical Physics*, Vol. 84, No. 2, 2011.